

Author's Accepted Manuscript

A mathematical model to simulate the cardiotocogram during labor, part B: parameter estimation and simulation of variable decelerations

Germaine J.L.M. Jongen, M. Beatrijs van der Hout-van der Jagt, Frans N. van de Vosse, S. Guid Oei, Peter H.M. Bovendeerd



PII: S0021-9290(16)30139-7S0021-9290(16)30110-5
DOI: <http://dx.doi.org/10.1016/j.jbiomech.2016.01.046>
Reference: BM7575

To appear in: *Journal of Biomechanics*

Received date: 20 January 2016

Accepted date: 28 January 2016

Cite this article as: Germaine J.L.M. Jongen, M. Beatrijs van der Hout-van de Jagt, Frans N. van de Vosse, S. Guid Oei and Peter H.M. Bovendeerd, A mathematical model to simulate the cardiotocogram during labor, part B parameter estimation and simulation of variable decelerations, *Journal of Biomechanics*, <http://dx.doi.org/10.1016/j.jbiomech.2016.01.046>

This is a PDF file of an unedited manuscript that has been accepted for publication. As a service to our customers we are providing this early version of the manuscript. The manuscript will undergo copyediting, typesetting, and review of the resulting galley proof before it is published in its final citable form. Please note that during the production process errors may be discovered which could affect the content, and all legal disclaimers that apply to the journal pertain.

A mathematical model to simulate the cardiotocogram during labor, part B: parameter estimation and simulation of variable decelerations

Germaine J.L.M. Jongen^{a,b,*},
M. Beatrijs van der Hout-van der Jagt^{a,b},
Frans N. van de Vosse^a, S. Guid Oei^{b,c},
Peter H.M. Bovendeerd^a

^a*Department of Biomedical Engineering, Eindhoven University of Technology,
Eindhoven, The Netherlands*

^b*Department of Gynecology and Obstetrics, Máxima Medical Center, Veldhoven,
The Netherlands*

^c*Department of Electrical Engineering, Eindhoven University of Technology,
Eindhoven, The Netherlands*

Word count: about 3970 words, excluding equations

* Corresponding author.

Address for correspondence:

Department of Biomedical Engineering
Eindhoven University of Technology
PO Box 513
5600 MB Eindhoven, The Netherlands
g.j.l.m.jongen@tue.nl

Abstract

During labor and delivery the cardiotocogram (CTG), the combined registration of fetal heart rate (FHR) and uterine contractions, is used to monitor fetal well-being. In part A of our study we introduced a new mathematical computer model for CTG simulation in order to gain insight into the complex relation between these signals. By reducing model complexity and by using physically more realistic descriptions, this model was improved with respect to our previous model.

Aim of part B of this study is to gain insight into the cascade from uterine contractions causing combined uterine flow reduction and umbilical cord compression, resulting in blood and oxygen pressure variations, which lead to changes in FHR via the baro- and chemoreflex. In addition, we extensively describe and discuss the estimation of model parameter values.

Simulation results are in good agreement with sheep data and show the ability of the model to describe variable decelerations. Despite reduced model complexity, parameter estimation still remains difficult due to limited clinical data.

Key words: fetal heart rate, umbilical cord compression, baroreflex, chemoreflex, computer simulation model

1 Introduction

In part A of our paper (Jongen et al., 2016a) we gave an overview of a new cardiotocogram (CTG) simulation model. Compared to our previous model (van der Hout-van der Jagt et al., 2012, 2013a,b) the complexity of some sub-
 5 models was reduced and the physical basis for the description of other submodels was enhanced. It was shown that the model was able to simulate realistic FHR decrease in response to uterine flow reduction as induced by uterine contractions.

In this part the model is used to gain insight into the mechanism of variable
 10 FHR decelerations which are caused by umbilical cord compressions, that mostly occur during uterine contractions during labor (Freeman et al., 2012). Variable decelerations are defined as an abrupt FHR decrease of more than 15 bpm, with a maximum time delay of 30 s between onset of the deceleration and FHR nadir, and a duration of less than 2 minutes (Macones et al., 2008;
 15 Robinson, 2008). In addition, the effect of varying amplitude and duration of uterine contractions on the CTG is investigated. We also compare model output with data of sheep experiments in which the umbilical cord was temporarily blocked by use of an occluder (Itskovitz et al., 1983). Although model complexity was reduced, parameter estimation is difficult due to the limited
 20 clinical data. Therefore, we will extensively describe and discuss estimation of

these parameter values.

The new model is intended to be used to gain insight into the regulation of FHR during labor and delivery. For use as a clinical decision support tool, the model should be made patient-specific. This is a challenging task in view of the limited availability of clinical data and the limited time span for model analysis during labor. Use as an educational tool would be a more realistic next step.

2 Material & Methods

The model is extensively described in part A of our study (Jongen et al., 2016a). In part B we extend the model in order to simulate combined uterine blood flow reduction and umbilical cord compression induced by contractions. Besides an overview of model parameter estimation is given.

2.1 Model extension

Since during cord compression the umbilical vein and arteries are exposed to large changes in transmural pressure, the corresponding resistances, R_{umv} and R_{uma} respectively, are modeled as function of transmural pressure p_{tm} (part A, eq. 6). Parameter values are chosen such that first the umbilical vein will be closed, followed by the umbilical arteries at higher external umbilical pressures, see table 1.

The transmural pressure of the umbilical vein $p_{tm,umv}$ and umbilical arteries $p_{tm,uma}$ is determined as the mean absolute pressure of the two neighboring blood compartments minus the external pressure:

$$\begin{aligned} p_{tm,umv} &= \frac{p_{villi} + p_{ven}}{2} - (p_{ut} + p_{um}) \\ p_{tm,uma} &= \frac{p_{villi} + p_{art}}{2} - (p_{ut} + p_{um}) \end{aligned} \quad (1)$$

where the external pressure consists of the uterine pressure p_{ut} , that acts on the whole fetus, plus an extra pressure p_{um} , caused by umbilical cord compression.

The degree of cord compression depends on the contraction intensity, fetal position, stage of labor, etc. The effect of these random variables is modeled through a weighting factor w_{um} [-], relating p_{ut} to the external pressure on the umbilical cord p_{um} :

$$p_{um} = w_{um}(p_{ut} - p_{rest}), w_{um} \geq 0 \quad (2)$$

with p_{rest} uterine resting pressure.

50 2.2 Parameter estimation

Due to the limited available human fetal data, parameter estimation is difficult. For this reason parameter estimation is extensively described. Fetal cardiovascular parameters were obtained from literature and set to values of a 3.5 kg term human fetus. If human data were not available, fetal sheep data
 55 were used to derive the parameters. Some parameter values were set to obtain the desired model responses. Parameter choices are briefly explained below, all parameter values can be found in table 1 to 3 of part A.

2.2.1 Feto-maternal hemodynamics

Fetal combined ventricular output q_{CO} was aimed at 450 ml/min/kg (Kiserud et al.,
 60 2006; Parer, 1997; Rudolph, 2009; van Mieghem et al., 2009), ejection fraction EF at 0.67 (Schmidt et al., 1995), and heart rate at 135 bpm (part A, table 1a). Mean arterial transmural blood pressure $p_{tm,a}$ and mean transmural venous blood pressure $p_{tm,v}$ were set to 45 mmHg (Itskovitz et al., 1983; Struijk et al., 2008; Thornburg & Morton, 1986; Unno et al., 1999) and
 65 3 mmHg (Johnson et al., 2000; Rudolph, 2009; Thornburg & Morton, 1986) respectively. Fetal blood volume was reported to be about 75 ml/kg (Linderkamp et al., 1978; Usher et al., 1963; Yao et al., 1969), which is about two third of total fetoplacental blood volume (Yao et al., 1969). Therefore, the latter volume was set to 110 ml/kg, which is in accordance with Schwarz (Schwarz & Galinkin,
 70 2003). Total microcirculation blood volume was computed from Guyton et al. (Guyton & Hall, 2006) and set to 8% of fetal body blood volume, which was distributed over cerebral (14%) (Cetin et al., 2008; Hofman, 1983) and tissue microcirculation (86%). Average cardiac cavity volume follows from q_{CO} , EF and FHR and equals 11.7 ml. The remainder of the body blood volume was
 75 distributed over the systemic fetal arteries (1/6) and veins (5/6). Based on geometric considerations (Di Naro et al., 2001; Link et al., 2007; Walker & Pye, 1960) blood volume of the umbilical circulation was divided between the placental villi (65%), umbilical arteries (10%) and vein (25%). Since for the umbilical arteries and vein no separate compartments were included in the model,
 80 these blood volumes were added to the systemic arteries and veins respectively.

Maternal cardiovascular parameters were based on pregnancy-related changes as described in literature (part A, table 1b). Target values for $p_{tm,a}$ and $p_{tm,v}$ were set to 80 mmHg (Clapp & Capeless, 1997; Geva et al., 1997; Katz et al., 1978) and 5 mmHg (Murray, 2007) respectively. During pregnancy, heart
 85 rate HR increases up to a target value of 80 bpm (Clapp & Capeless, 1997;

Geva et al., 1997; Katz et al., 1978; Rubler et al., 1977), while the cardiac output (Abbas et al., 2005; Clapp & Capeless, 1997; Katz et al., 1978; Longo, 1983) and blood volume (Abbas et al., 2005; Longo, 1983) both increase by 40%. In our model cardiac output and total blood volume were set to 7 l/min and 7 l, respectively. Ejection fraction was set to a value of 0.67 (Clapp & Capeless, 1997; Geva et al., 1997; Katz et al., 1978). Intervillous space volume was chosen to be 175 ml (Benirschke et al., 2006; Mayhew, 1996; Rainey & Mayhew, 2010), while the volume of the tissue microcirculation was chosen to be 8% of total maternal blood volume (Guyton & Hall, 2006). Average left ventricular blood volume follows from q_{CO} , EF and HR and equals 87.5 ml. Like in the fetus, the remainder of the blood volume was distributed over systemic arteries (1/6) and veins (5/6). Parameters p_1 and V_{max} , defining the relation between IVS volume and transmural blood pressure as described by eq. 3 of part A, were determined by assuming that $p_0 = p_{ref}$, where p_{ref} is the reference transmural IVS blood pressure in steady state. Then it follows that:

$$V_{max} = 2 \cdot V_{IVS}(p_{ref})$$

Finally p_1 was determined by assuming that IVS compliance is maximal at p_{ref} , meaning that:

$$p_1 = \frac{V_{max}}{\pi \cdot C_{IVS,max}}$$

For $C_{IVS,max}$ we chose a similar value as for the placental villi (2.4 ml/mmHg).

For both fetus and mother target values of blood flows and pressure were used to estimate resistances and compliances. We chose umbilical cord flow to be 25% of q_{CO} , in agreement with literature data that range from 15 and 34% of q_{CO} (Acharya et al., 2005; Kiserud et al., 2006; Link et al., 2007; Parer, 1997; Rudolph, 2009). The fraction of cardiac output going to the fetal brain was estimated by use of a fractional brain mass of 14% (Cetin et al., 2008; Hofman, 1983) and by the estimation that oxygen metabolism per gram tissue, and thus also blood flow per gram tissue, should be twice as high in brain tissue compared to peripheral tissues. This means that 21% of total cardiac output goes to the brain and 54% to the fetal tissues, which is in accordance with Rudolph (Rudolph, 2009). In the mother about 10% of the cardiac output is directed to the uterine circulation (Flo et al., 2010; Parer, 1997; Vorherr, 1975), of which 70-90% is directed to the IVS (Parer, 1997; Rosenfeld, 1984; Wang & Zhao, 2010). Hence we chose 9% of q_{CO} to be directed to the IVS, while 91% is directed to the other maternal tissues.

For the fetal and maternal tissues and fetal brain 95% of the total resistance was assigned to the microcirculation arteries, while 5% was assigned to the microcirculation veins. In the umbilical circulation, the arterial resistance fraction was set to 60%, to obtain a blood pressure of about 20 mmHg in the placental villi (Huikeshoven et al., 1980). In the uterine circulation this frac-

tion was set to 80%, in order to obtain an IVS pressure of about 60-70 mmHg
 125 below mean arterial pressure (Ramsey et al., 1959). Except for the placental
 villi and IVS, compliances were estimated assuming that 70% of the volume
 in the reference state contributes to the unstressed volume. For the cerebral
 and tissue microcirculation, unstressed volume fraction was set to 90%. The
 compliance in the placental villi was set to 2.4 ml/mmHg (Assad et al., 2001;
 130 Huikeshoven et al., 1980).

Initial values of V_{ed} and V_{ee} were calculated from target values of q_{CO} , EF and
 FHR. $V_{min,0}$ was chosen to be equal to V_{ee} , while $V_{max,0}$ was set to 0. Finally,
 E_{max} could be calculated as the slope of a line through the data points (V_{ee} ,
 $p_{tm,a}$) and ($V_{max,0}$, 0), while E_{min} was calculated as the slope of a line through
 135 (V_{ed} , $p_{tm,v}$) and ($V_{min,0}$, 0).

2.2.2 Oxygen distribution

The oxygen diffusion coefficient in the placenta was set to 0.082 ml O₂/(s·mmHg)
 (part A, table 2) such that in steady state a fetal umbilical arterial oxygen
 pressure of 18.5 mmHg was obtained (Acharya & Sitras, 2009; Link et al.,
 140 2007; Sjöstedt et al., 1960). Fetal oxygen metabolism was set to be 8 ml
 O₂/(min·kg) (Acharya & Sitras, 2009; Bonds et al., 1986) and divided over
 cerebral metabolism (28%) and tissue metabolism (72%). We chose a thresh-
 old value of 5 mmHg for cerebral oxygen metabolism ($pO_{2,th,cer,f}$) (Jones et al.,
 1977) and 10 mmHg for the peripheral tissues, where the latter value corre-
 145 sponds to about 50% of the steady-state oxygen concentration, based on Sá
 Couto (Sá Couto et al., 2002).

Maternal oxygen consumption was set to 600 ml O₂/min. The oxygen pressure
 in the air was set to 160 mmHg, while target maternal arterial oxygen pressure
 was set to 98 mmHg. Combination of this oxygen pressure difference and
 150 total feto-maternal oxygen metabolism yielded a pulmonary oxygen diffusion
 coefficient of 0.169 ml O₂/(s·mmHg). Since in the current study maternal
 oxygenation was kept constant, an oxygen metabolism threshold was irrelevant
 for the maternal model.

Fetal and maternal parameter values defining the relation between cO_2 and
 155 pO_2 were chosen as described by Sá Couto (Sá Couto et al., 2002).

2.2.3 Regulation

Cerebral autoregulation

For the cerebral autoregulation the value of γ , indicating how well the cerebral
 resistance can adapt to variations in arterial oxygen content, was estimated

by use of Peeters (Peeters et al., 1979) and set to a value of 0.5. The cerebral resistance can maximally decrease by 50%, which means that cerebral blood flow can increase with a factor of 2. Finally, the time constant $\tau_{R_{cera}}$ was chosen to be 10 s according to Ursino (Ursino & Magosso, 2000).

Central regulation

For the baroreceptor and chemoreceptor outputs (part A, eq. 21) the parameters η_1 and η_2 follow from the condition that $r(y = y_{ref}) = 0$ and from the (desired) slope at the reference point ($y = y_{ref}$):

$$\eta_1 = \ln\left(\frac{-r_{min}}{r_{max} - r_{min}}\right) \quad (3)$$

$$\left.\frac{dr^*(y)}{dy}\right|_{y=y_{ref}} = \eta_2 \cdot \eta_1 e^{\eta_1} (r_{max} - r_{min}) \quad (4)$$

Baroreceptor parameters were obtained by scaling the relation as described by Ursino (Ursino & Magosso, 2000) to fetal values and normalizing it to a range between -1 and 1 (part A, table 3). Baroreceptor sensitivity in the fetus is reduced by a factor two as compared to the adult (Dawes et al., 1980). Parameter values of the Gompertz function were chosen such that the relation between baroreceptor input $p_{tm,a}$ and output r_b closely resembled the scaled response of Ursino. Parameter values for the chemoreceptor response were chosen such that a reference contraction of 60 s with a pressure amplitude of 70 mmHg would lead to a maximum FHR deceleration of about 3 bpm for uterine flow reduction alone and about 50 bpm for combined uterine flow reduction and umbilical cord compression. The values of the effector gains k and efferent weighting factors w were also chosen to obtain the desired effects in FHR (part A, table 3). For all effectors time delays D and low pass filter time constants τ were obtained from Ursino (Ursino & Magosso, 2000) (part A, table 3).

2.2.4 Uterine and umbilical blood vessel compressions

In the relation between transmural blood pressure and vessel resistance (part A, eq. 6) R_0 was chosen such that $R(p_{th}) = R_{ref}$, with p_{th} the transmural pressure below which the blood vessel resistance starts to increase and R_{ref} is the reference resistance in steady state. For the uterine vein p_0 and p_1 were chosen such that a contraction with a uterine pressure amplitude of 60 mmHg and a duration of 60 s would result in a 60% blood flow reduction through the uterine artery (Janbu & Nesheim, 1987) (part A, table 1b). In our model, the uterine arteries are not subjected to increasing uterine pressure. Parameter settings for the umbilical cord resistances were found by simulating the sheep experiments in which initial fetal blood volume changes were measured during umbilical cord compressions with increasing external pressures (Cooper & Greenfield,

1949). The umbilical vein is totally closed if the external pressure exceeds 40 mmHg, while the umbilical arteries are compressed over a pressure range of 40 to 90 mmHg (see table 1).

2.3 Model simulations

200 We simulated combined uterine flow reduction and umbilical cord compression in term pregnancy by setting $w_{um} = 1$ in (2). A reference contraction with a duration (T_{con}) of 60 s and a pressure amplitude (p_{con}) of 70 mmHg with respect to the reference pressure (p_{rest}) of 15 mmHg was used. To illustrate the effect of regulation, simulations with and without central regulation and
205 autoregulation were performed. In addition, the effect of contraction intensity was investigated by changing contraction amplitude from 70 mmHg to 30 and 110 mmHg respectively, or contraction duration from 60 s to 30 and 120 s respectively.

The model was evaluated by use of sheep experiments in which umbilical cord
210 blood flow was temporarily reduced by use of an occluder (Itskovitz et al., 1983). The sheep experiments were simulated by linearly increasing the external pressure (p_{um}) on the cord over 5 s to a maximum level, which was maintained for 35 s, and reduced to zero over another 5 s, while keeping p_{ut} at the resting level. In order to obtain umbilical flow reductions of 25%, 50%,
215 75% or 100%, as presented by Itskovitz, maximum external pressure was set to a value of 25, 33, 41, or 90 mmHg, respectively. Umbilical vein and artery resistance, R_{umv} and R_{uma} respectively, were calculated by use of eq. 6 in part A.

3 Results

220 Figure 1 shows the scenario of combined uterine flow reduction and umbilical cord compression induced by a reference contraction of 60 s with a pressure amplitude of 70 mmHg. Initial values for this scenario are the same as for the scenario of uterine flow reduction alone, as described in part A. In addition,
225 figure 1 shows that umbilical blood flow is about 394 ml/min (panel B1) and that villous volume is 83 ml (panel B2). Note that blood pressures described in this section represent transmural blood pressures.

We first consider the simulation without regulation, indicated by the gray lines. During cord compression the external umbilical pressure rises (panel A1) and fetal blood pressure (panel A2) and arterial oxygen pressure (panel
230 A3) decrease. Without regulation, FHR will not be affected (panel A4). If

we now look into more detail (column B), we observe that first umbilical venous flow reduces to near zero (panel B1) and that the placental villi are filled via the umbilical arteries (panel B2). Once the umbilical arteries are compressed as well, villous volume remains more or less constant. This blood volume shift from fetus to placenta explains the drop in blood pressure (panel A2) that in turn causes a drop of blood flow through the fetal tissues and brain (panel B4). The reduction of umbilical blood flow decreases arterial, cerebral, and tissue oxygen levels (panel A3 and B3). Initially no difference is observed between the cerebral and tissue oxygen pressures. Later, cerebral oxygen pressure drops deeper than tissue oxygen pressure, which is due to the lower oxygen metabolism threshold value in the brain (part A, eq. 17). At the end of the occlusion umbilical cord vessels open again and all values will return back to normal levels. The regulation signals, as shown in column C, do not change if regulation is switched off.

In the situation with cardiovascular regulation, indicated by the black lines, the initial decrease in arterial blood pressure results in a decreased baroreceptor output (panel C1) that in turn causes an increase of the sympathetic, and decrease of the vagal efferent signal. This change is modified by the chemoreceptor-mediated increase of both efferent signals. The resulting efferent signals (panel C2) cause an initial drop of heart period (panel C4) and consequently an initial increase in FHR (panel A4). The ongoing decrease in oxygen pressure further increases chemoreceptor output (panel C1), stimulating both efferent signals (panel C2). The increased sympathetic response results in an increase of peripheral vascular resistance and cardiac contractility, while venous unstressed volume is reduced (panel C3). This leads to an increase of arterial blood pressure (panel A2) and baroreceptor output (panel C1). The weighted average of the chemo- and baroreceptor outputs now results in a similar time course of the vagal and sympathetic efferent signal (panel C2). Since vagal feedback on heart period is twice as strong as sympathetic feedback, FHR responds with a deceleration (panel A4). Comparison of panels A4 and C1 shows that the timing of the minimum FHR at about 1.3 min is dominated by the chemoreceptor response, while the timing of the second dip at 1.6 min is caused by the baroreceptor response. Finally, cerebral autoregulation decreases cerebral vascular resistance (panel C3), thereby increasing cerebral blood flow (panel B4). Together with flow reduction in the tissues caused by the increased peripheral resistance, this results in flow redistribution in favor of the fetal brain. As a consequence the drop in cerebral oxygen pressure is reduced compared to the unregulated case (panel B3).

In figure 2 the effect of variation in contraction amplitude and duration is shown. In general an increased or decreased contraction duration has a similar but opposite effect on pressures and FHR, while variation of amplitude has a nonlinear effect. When contraction amplitude is increased to 110 mmHg (column A) only minor changes are seen compared to the reference contraction.

When contraction amplitude is reduced to 30 mmHg (column B) umbilical
 275 vessels do not become fully blocked, hence less blood is stored in the villi,
 and thus the drop of arterial blood pressure is reduced. The drop of oxygen
 pressure is reduced since oxygen supply through venous umbilical flow contin-
 ues. FHR remains rather constant, because of the reduced baroreceptor and
 chemoreceptor response. If contraction duration is increased to 120 s (column
 280 C) the drop in arterial blood pressure is similar to that during the reference
 contraction. The increased FHR deceleration is mainly caused by the increased
 chemoreceptor feedback, in response to the lower oxygen levels. Finally, if con-
 traction duration is decreased to 30 s, less blood is stored in the villi, and the
 initial arterial pressure drop is reduced. Arterial oxygen pressure drops less
 285 deep, due to the shortened duration of umbilical cord compression. FHR drops
 less deep because of reduced baroreceptor and chemoreceptor feedback.

Figure 3 shows the relative variations in arterial oxygen pressure, blood pres-
 sure and FHR during different degrees of umbilical cord block as obtained from
 sheep data (Itskovitz et al., 1983) and from model simulations. Quantitatively,
 290 the simulation results agree well with the experimental data.

4 Discussion

Parameter estimation. Parameter estimations were described in section 2.2.
 The most important choices will be discussed here.

It has been reported that the baroreceptor sensitivity in the fetus is two to
 295 eight times lower than that in the adult (Dawes et al., 1980). In the model, we
 used a two-fold decrease with respect to settings for the adult, used by Ursino
 (Ursino & Magosso, 2000). With this setting, we observed an initial increase
 of FHR (clinically referred to as ‘shoulders’) when simulating variable decel-
 erations, which disappeared when further lowering baroreceptor sensitivity.

300 Clinically, most contractions that affect uterine blood flow alone, lead to re-
 ductions in FHR (‘late decelerations’) that do barely exceed the noise level of
 the FHR signal in a healthy fetus. In the model, we tuned parameter settings
 such that simulation of our reference contraction with uterine flow reduction
 alone yields an FHR deceleration of about 3 bpm. Due to the variable charac-
 305 ter of the FHR decelerations caused by combined uterine and umbilical flow
 reduction, there is no typical response for this ‘variable deceleration’ scenario.
 We chose a target value of 50 bpm during a reference contraction. Deeper
 decelerations can be reached if contractions duration or amplitude increases
 (figure 2).

310 Since oxygen pressure dropped by 1.5 mmHg in the former scenario, and by

6 mmHg in the latter scenario, chemoreceptor output had to increase steeply over a small arterial oxygen pressure interval. Finally, to obtain the desired results, the effector gains k were multiplied by a factor 6 with respect to Wesseling (Wesseling & Settels, 1985). This adaptation can partly be explained from the fact that in our regulation model the chemoreceptor was added and a larger reduction of FHR was desired. Simulation of other scenarios is needed to test the validity of these parameter settings. However, the clinical or experimental data to validate the model is limited.

Results. Simulation results show that oxygen levels drop more quickly during combined uterine and umbilical flow reduction (figure 1) compared to uterine flow reduction alone (part A, figure 3). This can be explained by the fact that during cord compression the fetus has no access to the IVS oxygen buffer, since oxygen cannot be transported from the placental villi into the fetus. Until the oxygen threshold is reached below which metabolic rate decreases, oxygen content drops linearly in time. Since the oxygen pressures reached are still in the linear range of the saturation curve, oxygen pressure also drops linearly. We observed that FHR increases before onset of the decelerations. This increase is clinically referred to as ‘shoulder’ (Murray, 2007; Essed et al., 2008; Parer, 1997). In the clinic these shoulders are often also observed at the end of the deceleration, however this effect was not obtained in the model, presumably due to the dominant sympathetically-induced blood pressure increase in our model. During a standard contraction the FHR decreases from baseline to nadir in about 26 s, which is in accordance with the clinical guidelines defining an abrupt decrease in FHR to occur within 30 s (Macones et al., 2008; Robinson, 2008). Furthermore, FHR reaches baseline levels again within 2 minutes. This is in accordance with literature (Macones et al., 2008; Robinson, 2008), although the final part of FHR return seems somewhat slow.

Simulation results of contraction variations (figure 2) show that oxygen pressure reduction depends on the duration and amplitude of the contraction, which will both increase during progression of labor. The time delay between onset and nadir of the FHR deceleration increases with increasing contraction amplitude or duration. The wide variation in the shapes of the FHR decelerations corresponds well with the clinical observation that umbilical cord occlusions have a variable character and are therefore called ‘variable’ decelerations. Clinically, these variations are also caused by variation in the position of the umbilical cord within the uterus. In the model this could be simulated by variation of the weighting factor w_{um} in (2). However, since random variation of this factor would complicate comparison of the results in the various scenarios, we kept this factor constant.

If we compare FHR signals obtained with the current model with the results of our previous model (van der Hout-van der Jagt et al., 2013b), we see that FHR decelerations are now preceded by a shoulder, which was not observed

in the previous model. This shoulder can partly be attributed to increased filling of the villi, due to the fact that the umbilical arteries remain patent, and partly to the stronger baroreceptor response in the current model.

The model generates estimates of many physiological signals, while in clinical practice only FHR can be measured continuously. To gain more insight into the complex pathway from uterine contractions to FHR changes, we also show signals that cannot be measured in the clinic. Since these intermediate signals cannot be compared to human data, we used sheep data on oxygen pressure and blood pressure to evaluate the model, noting that quantitative comparison with sheep data is difficult due to the differences between the ovine and human fetus. For example, in fetal lambs about 40-45% of the cardiac output is directed to the umbilical circulation (Jensen et al., 1991; Parer, 1997; Rudolph, 2009), while in the human fetus this is only 25%. Despite the differences between human and sheep fetuses, for the simulations of umbilical cord blocking, results were quantitatively in accordance with sheep experiments (figure 3).

Limitations. Although we reduced the number of model parameters to be estimated, it is still difficult to arrive at a unique set of model parameter settings from the limited experimental data presented in literature. Consequently, there may be different combinations of parameter choices which will lead to similar results. In future a sensitivity analysis should be performed in order to investigate which parameters dominate model response and should be determined very precisely and for which parameters a more general value can be used.

The model lacks the ability to describe short-term FHR variability, which is an important indicator of fetal distress in clinical practice. Addition of this variability would further improve applicability of the model for training purposes and clinical diagnosis and decision making.

The current model is intended to describe CTG signals during short-term hypoxia and to provide additional information on fetal oxygen status. To be able to describe the effects caused by stronger and longer contractions, humoral feedback has to be added to the model (Murray, 2007), and the shift of the fetal oxygen dissociation curve due to the changes in pH (Bohr effect) should be taken into account. Furthermore, cardiac metabolism and the effect of myocard hypoxia on FHR might be included in the model.

In the hemodynamic model of the fetus, the fetal heart is represented by a combined ventricle. To describe improved oxygen supply to the brain due to preferential blood flows, the combined ventricle might be replaced by a separate left and right ventricle.

Conclusion. With the improved model we were able to generate realistic

variable decelerations for the scenario of combined uterine and umbilical flow reduction. Parameter estimation of the simplified model remains difficult due to the limited availability of clinical and experimental data.

Conflict of interest statement

There are no conflicts of interest between the authors of this paper and other external researchers or organizations that could have inappropriately influenced this work.

Acknowledgements

This research was performed within the IMPULS perinatology framework.

References

- Abbas, A. E., Lester, S. J., & Connolly, H. (2005). Pregnancy and the cardiovascular system. *Int J Cardiol*, *98*, 179–189.
- Acharya, G., & Sitras, V. (2009). Oxygen uptake of the human fetus at term. *Acta Obstet Gynecol Scand*, *88*, 104–109.
- Acharya, G., Wilsgaard, T., Rosvold Berntsen, G. K., Maltau, J. M., & Kiserud, T. (2005). Reference ranges for umbilical vein blood flow in the second half of pregnancy based on longitudinal data. *Prenat Diagn*, *25*, 99–111.
- Assad, R. S., Lee, F. Y., & Hanley, F. L. (2001). Placental compliance during fetal extracorporeal circulation. *J Appl Physiol*, *90*, 1882–1886.
- Benirschke, K., Kaufmann, P., & Baergen, R. N. (2006). *Pathology of the Human Placenta*. (5th ed.). Springer, New York.
- Bonds, D. R., Crosby, L. O., Cheek, T. G., Hgerdal, M., Gutsche, B. B., & Gabbe, S. G. (1986). Estimation of human fetal-placental unit metabolic rate by application of the Bohr principle. *J Dev Physiol*, *8*, 49–54.
- Cetin, I., Boito, S., & Radaelli, T. (2008). Evaluation of fetal growth and fetal well-being. *Semin Ultrasound CT MRI*, *29*, 136–146.
- Clapp, J. F., 3rd, & Capeless, E. (1997). Cardiovascular function before, during, and after the first and subsequent pregnancies. *Am J Cardiol*, *80*, 1469–1473.
- Cooper, K. E., & Greenfield, A. D. M. (1949). A method for measuring the blood flow in the umbilical vessels. *J Physiol*, *108*, 167–176.
- Dawes, G. S., Johnston, B. M., & Walker, D. W. (1980). Relationship of arterial pressure and heart rate in fetal, new-born and adult sheep. *J Physiol*, *309*, 405–417.
- Di Naro, E., Ghezzi, F., Raio, L., Franchi, M., & D'Addario, V. (2001). Umbilical cord morphology and pregnancy outcome. *Eur J Obstet Gynecol Reprod Biol*, *96*, 150–157.

- Essed, G. G. M., Nijhuis, J. G., van Geijn, H. P., & Visser, G. H. A. (2008). Kenmerken van een cardiotocogram. In J. G. Nijhuis, G. G. M. Essed, H. van Geijn, & G. H. A. Visser (Eds.), *Foetale bewaking* chapter 4. (pp. 51–58). Reed Business Education, Amsterdam. (2nd ed.).
- 435 Flo, K., Wilsgaard, T., Vårtun, A., & Acharya, G. (2010). A longitudinal study of the relationship between maternal cardiac output measured by impedance cardiography and uterine artery blood flow in the second half of pregnancy. *BJOG*, *117*, 837–844.
- 440 Freeman, R. K., Garite, T. J., Nageotte, M. P., & Miller, L. A. (2012). *Fetal Heart Rate Monitoring*. (4th ed.). Lippincott Williams & Wilkins, Philadelphia.
- Geva, T., Mauer, M. B., Striker, L., Kirshon, B., & Pivarnik, J. M. (1997). Effects of physiologic load of pregnancy on left ventricular contractility and remodeling. *Am Heart J*, *133*, 53–59.
- 445 Guyton, A. C., & Hall, J. E. (2006). *Textbook of medical physiology*. (11th ed.). Elsevier Saunders, Philadelphia.
- Hofman, M. A. (1983). Evolution of brain size in neonatal and adult placental mammals: a theoretical approach. *J Theor Biol*, *105*, 317–332.
- Huikeshoven, F., Coleman, T. G., & Jongsma, H. W. (1980). Mathematical model of the fetal cardiovascular system: the uncontrolled case. *Am J Physiol*, *239*, R317–R325.
- 450 Itskovitz, J., LaGamma, E. F., & Rudolph, A. M. (1983). Heart rate and blood pressure responses to umbilical cord compression in fetal lambs with special reference to the mechanism of variable deceleration. *Am J Obstet Gynecol*, *147*, 451–457.
- 455 Janbu, T., & Nesheim, B. I. (1987). Uterine artery blood velocities during contractions in pregnancy and labour related to intrauterine pressure. *Br J Obstet Gynaecol*, *94*, 1150–1155.
- Jensen, A., Roman, C., & Rudolph, A. M. (1991). Effects of reducing uterine blood flow on fetal blood flow distribution and oxygen delivery. *J Dev Physiol*, *15*, 309–323.
- 460 Johnson, P., Maxwell, D. J., Tynan, M. J., & Allan, L. D. (2000). Intracardiac pressures in the human fetus. *Heart*, *84*, 59–63.
- Jones, M. D., Jr, Sheldon, R. E., Peeters, L. L., Meschia, G., Battaglia, F. C., & Makowski, E. L. (1977). Fetal cerebral oxygen consumption at different levels of oxygenation. *J Appl Physiol Respir Environ Exerc Physiol*, *43*, 1080–1084.
- 465 Jongen, G. J. L. M., van der Hout-van der Jagt, M. B., van de Vosse, F. N., Oei, S. G., & Bovendeerd, P. H. M. (2016a). A mathematical model to simulate the cardiotocogram during labor, part A: model setup and simulation of late decelerations. Submitted to J Biomech.
- 470 Katz, R., Karliner, J. S., & Resnik, R. (1978). Effects of a natural volume overload state (pregnancy) on left ventricular performance in normal human subjects. *Circulation*, *58*, 434–441.
- 475 Kiserud, T., Ebbing, C., Kessler, J., & Rasmussen, S. (2006). Fetal cardiac

- output, distribution to the placenta and impact of placental compromise. *Ultrasound Obstet Gynecol*, 28, 126–136.
- Linderkamp, O., Versmold, H. T., Messow-Zahn, K., Müller-Holve, W., Riegel, K. P., & Betke, K. (1978). The effect of intra-partum and intra-uterine asphyxia on placental transfusion in premature and full-term infants. *Eur J Pediatr*, 127, 91–99.
- Link, G., Clark, K. E., & Lang, U. (2007). Umbilical blood flow during pregnancy: evidence for decreasing placental perfusion. *Am J Obstet Gynecol*, 196, 489e1–489e7.
- Longo, L. D. (1983). Maternal blood volume and cardiac output during pregnancy: a hypothesis of endocrinologic control. *Am J Physiol*, 245, R720–R729.
- Macones, G. A., Hankins, G. D. V., Spong, C. Y., Hauth, J., & Moore, T. (2008). The 2008 National Institute of Child Health and Human Development workshop report on electronic fetal monitoring: update on definitions, interpretation, and research guidelines. *J Obstet Gynecol Neonatal Nurs*, 37, 510–515.
- Mayhew, T. M. (1996). Patterns of villous and intervillous space growth in human placentas from normal and abnormal pregnancies. *Eur J Obstet Gynecol Reprod Biol*, 68, 75–82.
- Murray, M. (2007). *Antepartal and intrapartal fetal monitoring*. (3rd ed.). Springer Publishing Company, New York.
- Parer, J. T. (1997). *Handbook of fetal heart rate monitoring*. (2nd ed.). W.B. Saunders Co. Philadelphia.
- Peeters, L. L. H., Sheldon, R. E., Jones Jr., M. D., Makowski, A. L., & Meschia, G. (1979). Blood flow to fetal organs as a function of arterial oxygen content. *Am J Obstet Gynecol*, 135, 637–646.
- Rainey, A., & Mayhew, T. M. (2010). Volumes and numbers of intervillous pores and villous domains in placentas associated with intrauterine growth restriction and/or pre-eclampsia. *Placenta*, 31, 602 – 606.
- Ramsey, E. M., Corner, G. W., Jr, Long, W. N., & Stran, H. M. (1959). Studies of amniotic fluid and intervillous space pressures in the rhesus monkey. *Am J Obstet Gynecol*, 77, 1016–1027.
- Robinson, B. (2008). A review of NICHD standardized nomenclature for cardiotocography: the importance of speaking a common language when describing electronic fetal monitoring. *Rev Obstet Gynecol*, 1, 56–60.
- Rosenfeld, C. R. (1984). Consideration of the uteroplacental circulation in intrauterine growth. *Semin Perinatol*, 8, 42–51.
- Rubler, S., Damani, P. M., & Pinto, E. R. (1977). Cardiac size and performance during pregnancy estimated with echocardiography. *Am J Cardiol*, 40, 534–540.
- Rudolph, A. M. (2009). *Congenital Diseases of the Heart: Clinical-Physiological Considerations*. (3rd ed.). Wiley-Blackwell, Oxford.
- Sá Couto, P. M., van Meurs, W. L., Bernardes, J. F., Marques de Sá, J. P., & Goodwin, J. A. (2002). Mathematical model for educational simulation of

- the oxygen delivery to the fetus. *Control Eng Prac*, 10, 59–66.
- Schmidt, K. G., Silverman, N. H., & Hoffman, J. I. E. (1995). Determination of ventricular volumes in human fetal hearts by two-dimensional echocardiography. *Am J Cardiol*, 76, 1313–1316.
- 525 Schwarz, U., & Galinkin, J. L. (2003). Anesthesia for fetal surgery. *Semin Pediatr Surg*, 12, 196–201.
- Sjöstedt, S., Rooth, G., & Caligara, F. (1960). The oxygen tension of the blood in the umbilical cord and the intervillous space. *Arch Dis Child*, 35, 529–533.
- 530 Struijk, P. C., Mathews, V. J., Loupas, T., Stewart, P. A., Clark, E. B., Steegers, E. A. P., & Wladimiroff, J. W. (2008). Blood pressure estimation in the human fetal descending aorta. *Ultrasound Obstet Gynecol*, 32, 673–681.
- Thornburg, K. L., & Morton, M. J. (1986). Filling and arterial pressures as determinants of left ventricular stroke volume in fetal lambs. *Am J Physiol*, 535 251, H961–H968.
- Unno, N., Wong, C. H., Jenkins, S. L., Wentworth, R. A., Ding, X. Y., Li, C., Robertson, S. S., Smotherman, W. P., & Nathanielsz, P. W. (1999). Blood pressure and heart rate in the ovine fetus: ontogenic changes and effects of fetal adrenalectomy. *Am J Physiol*, 276, H248–H256.
- 540 Ursino, M., & Magosso, E. (2000). Acute cardiovascular response to isocapnic hypoxia. I. A mathematical model. *Am J Physiol Heart Circ Physiol*, 279, H149–H165.
- Usher, R., Shephard, M., & Lind, J. (1963). The blood volume of the newborn infant and placental transfusion. *Acta Paediatr*, 52, 497–512.
- 545 van der Hout-van der Jagt, M. B., Jongen, G. J. L. M., Bovendeerd, P. H. M., & Oei, S. G. (2013b). Insight into variable fetal heart rate decelerations from a mathematical model. *Early Hum Dev*, 89, 361–369.
- van der Hout-van der Jagt, M. B., Oei, S. G., & Bovendeerd, P. H. M. (2012). A mathematical model for simulation of early decelerations in the cardiotocogram during labor. *Med Eng Phys*, 34, 579–589.
- 550 van der Hout-van der Jagt, M. B., Oei, S. G., & Bovendeerd, P. H. M. (2013a). Simulation of reflex late decelerations in labor with a mathematical model. *Early Hum Dev*, 89, 7–19.
- 555 van Mieghem, T., DeKoninck, P., Steenhaut, P., & Deprest, J. (2009). Methods for prenatal assessment of fetal cardiac function. *Prenat Diagn*, 29, 1193–1203.
- Vorherr, H. (1975). Placental insufficiency in relation to postterm pregnancy and fetal postmaturity. Evaluation of fetoplacental function; management of the postterm gravida. *Am J Obstet Gynecol*, 123, 67–103.
- 560 Walker, C. W., & Pye, B. G. (1960). The length of the human umbilical cord: a statistical report. *Br Med J*, 1, 546–548.
- Wang, Y., & Zhao, S. (2010). *Vascular Biology of the Placenta*. Morgan & Claypool.
- 565 Wesseling, K. H., & Settels, J. J. (1985). Baromodulation explains short-term

blood pressure variability. In J. F. Orlebeke, G. Mulder, & L. J. P. van Doornen (Eds.), *Psychophysiology of cardiovascular control: models, methods, and data* (pp. 69–97). Plenum Press, New York volume 26.

570 Yao, A. C., Moinian, M., & Lind, J. (1969). Distribution of blood between infant and placenta after birth. *Lancet*, 294, 871–873.

Accepted manuscript

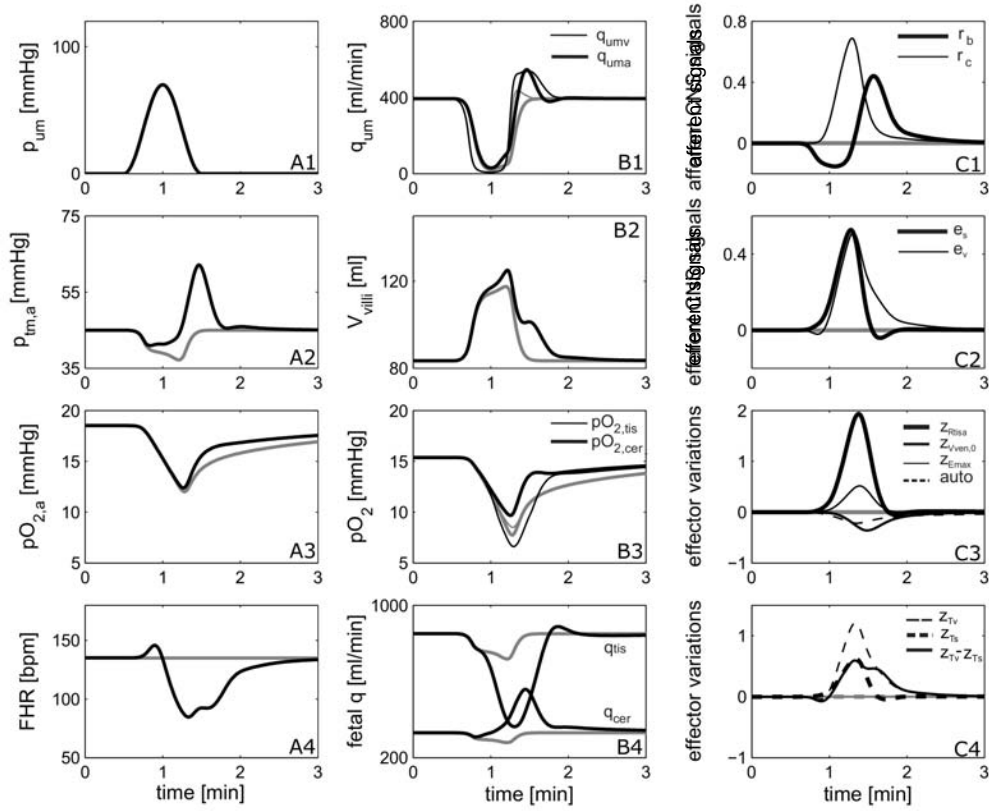


Figure 1. Simulation results for a standard uterine contraction of 60 s with an amplitude of 70 mmHg. From top to bottom signals in column A represent external umbilical pressure (p_{um}); mean arterial transmural blood pressure ($p_{tm,a}$); arterial oxygen pressure ($pO_{2,a}$); and FHR. In column B signals represent blood flow through the umbilical vein and arteries (q_{umv} and q_{uma} , respectively); villous blood volume (V_{villi}); tissue and cerebral oxygen pressure ($pO_{2,tis}$ and $pO_{2,cer}$, respectively); and fetal tissue and cerebral blood flow (q_{tis} and q_{cer} , respectively). Dimensionless signals in column C represent baro- and chemoreceptor outputs (r_b and r_c , respectively); sympathetic and vagal efferent signals (e_s and e_v , respectively); relative effector changes z for peripheral vascular resistance (R_{tisa}), venous unstressed volume ($V_{ven,0}$), and cardiac contractility (E_{max}), while the ‘auto’ signal represents the relative change of the autoregulated cerebral resistance (R_{cera}); and finally relative vagally- and sympathetically-induced heart period changes (z_{Tv} and z_{Ts} , respectively), and the difference between both ($z_{Tv} - z_{Ts}$). (Note the change in axes compared to figure 3 in part A.)

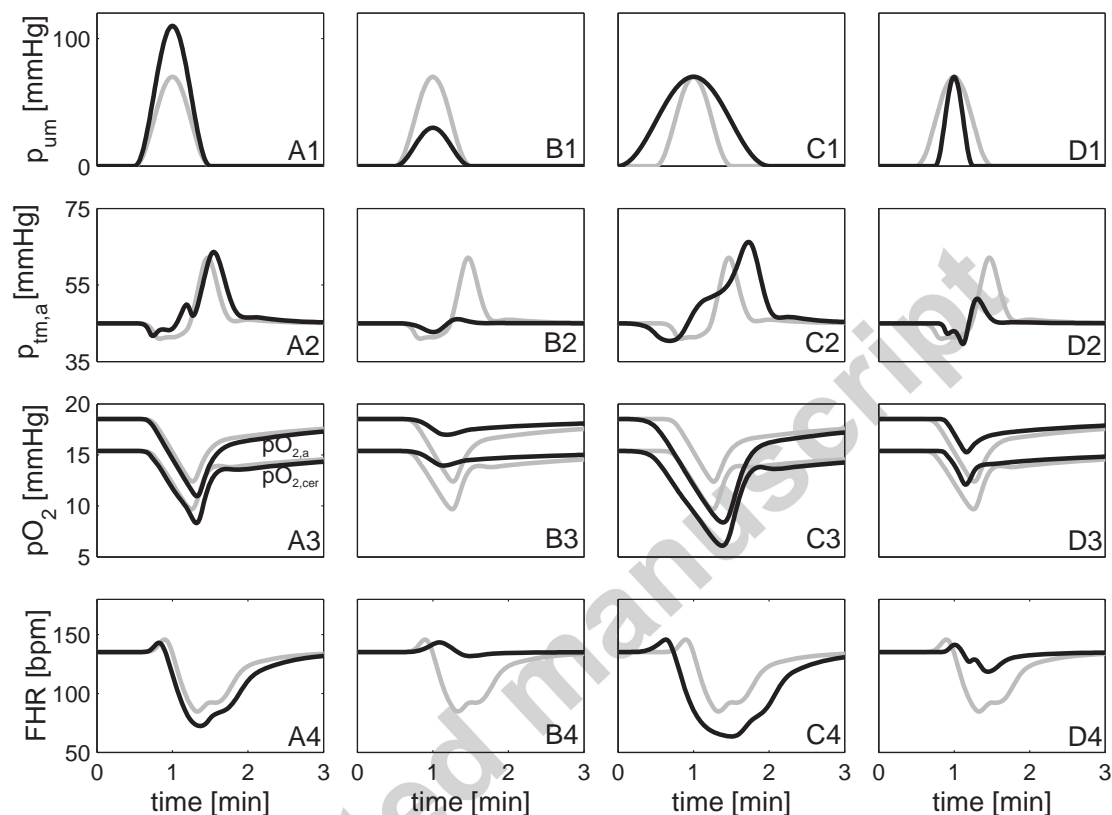


Figure 2. Simulation results for uterine contractions with varying contraction amplitude and duration. With respect to the reference contraction with a duration of 60 s and an amplitude of 70 mmHg, indicated in light gray, contraction amplitude was set to 110 mmHg (column A) or 30 mmHg (column B), or contraction duration was set to 120 s (column C), or 30 s (column D). The signals shown in each column are similar to the signals shown in column A of figure 1.

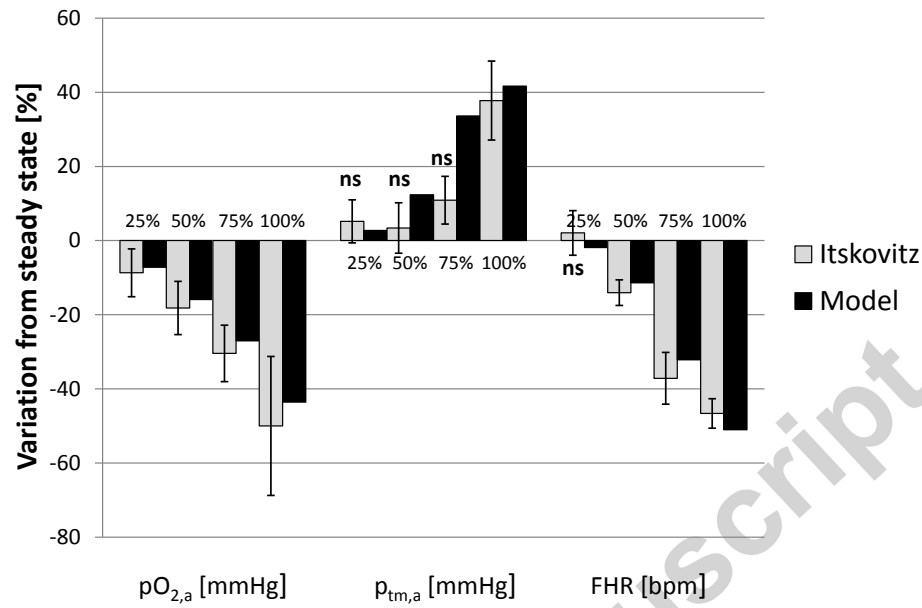


Figure 3. Results from simulations of umbilical cord occlusion, in comparison to experimental results from sheep studies (Itskovitz et al., 1983). From left to right: relative variations in arterial oxygen pressure ($pO_{2,a}$), transmural arterial blood pressure ($p_{tm,a}$), and FHR. N.B.: 'ns' indicates that the relative flow reduction does not result in a significant variation with respect to the steady-state value.

Table 1
Umbilical vein and artery resistance parameters.

Parameter	Value	Unit
$R_{0,umv}$	2.05	[mmHg·s/ml]
$p_{0,umv}$	-17	mmHg
$p_{1,umv}$	10	mmHg
$R_{0,uma}$	2.34	[mmHg·s/ml]
$p_{0,uma}$	-27	mmHg
$p_{1,uma}$	16	mmHg